

MODELING AND OUTDOOR CHARACTERIZATION OF TWO THIN-FILM PHOTOVOLTAIC MODULES: A CASE STUDY OF A-SI AND CIGS MODULES IN A SEMI-ARID CLIMATE ZONE

Hazim M. Mehdi^{a,b*}, Emad T. Hashim^b

^aCollege of Education, Al-Iraqia University, Baghdad 10053, Iraq

^bDepartment of Energy Engineering, University of Baghdad, Baghdad 10071, Iraq

Article history

Received

21 May 2024

Received in revised form

07 October 2024

Accepted

28 December 2024

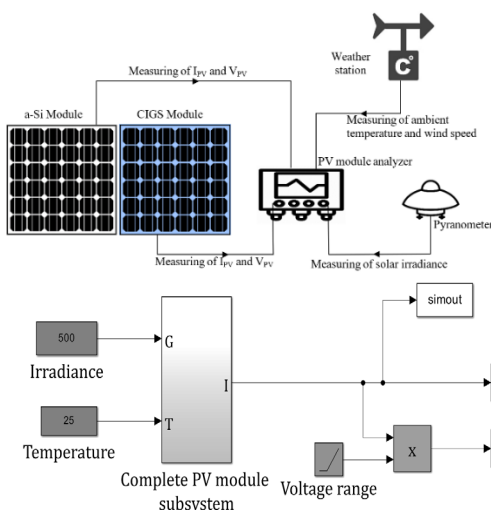
Published online

31 August 2025

*Corresponding author

hazem.m.mahdi@aliraqia.edu.iq

Graphical abstract



Abstract

Reliable modeling of photovoltaic (PV) module performance under field conditions is important for optimizing system design. This study evaluates two promising thin-film technologies, an amorphous silicon (a-Si) 5W module and copper indium gallium diselenide (CIGS) 7W module, under Baghdad's semi-arid climate over six months. Outdoor current-voltage and power-voltage curves were measured at irradiation levels of 500-1000 W/m² and module temperatures of 25-50°C. A validated five-parameter model was used to simulate module performance. At 1000 W/m² irradiation and 25°C, measurements showed maximum power outputs of 4.05W and 7.11W for the a-Si and CIGS modules respectively. The model predicted these values within 5% (3.9W) and 4% (7.37W). Model errors were below 10% for all test conditions. Specifically, at 500 W/m² and 50°C, measured powers were 1.75W (a-Si) and 3.11W (CIGS), while modeled outputs were 1.8W and 3.07W respectively. This analysis provides a comprehensive long-term experimental dataset and accurate modeling of these thin-film technologies under real Middle Eastern operating conditions. It can aid optimization of PV systems based on these promising thin-film technologies.

Keywords: Photovoltaics, Thin-film solar modules, Five-parameter model, Outdoor characterization.

© 2025 Penerbit UTM Press. All rights reserved

1.0 INTRODUCTION

Photovoltaic (PV) technology has emerged as a promising renewable energy option due to its ability to directly convert sunlight into electricity through the photovoltaic effect, without producing greenhouse gas emissions or other pollutants [1]. PV systems are composed of solar modules, which in turn, consist of interconnected solar cells arranged in series and parallel configurations to achieve desired voltage and current outputs. Solar cells can be designed as single-junction or multi-junction

components to absorb different ranges of the solar spectrum, with multi-junction cells offering higher absorption efficiency compared to single-junction counterparts [2]. PV systems can be broadly categorized into three generations: first generation includes traditional crystalline silicon modules, second generation encompasses thin-film technologies like amorphous silicon (a-Si), cadmium telluride (CdTe), and copper indium gallium diselenide (CIGS), while third generation consists of emerging thin-film technologies such as organic and inorganic solar cells [3].

The performance and energy yield of PV modules are influenced by various intrinsic and extrinsic factors, including solar irradiance levels, cell temperature, module technology, and environmental conditions [4]. Considerable research efforts have been devoted to investigating the temperature dependence of different PV technologies and its impact on efficiency and output power. Virtuani et al. [5] conducted comprehensive indoor measurements on several thin-film PV technologies, including single-junction and multi-junction a-Si, CdTe, and CIGS. Their findings revealed that the a-Si device exhibited the lowest temperature coefficient for maximum power of $-0.13\%/^{\circ}\text{C}$, while CdTe and CIGS modules showed coefficients of $-0.21\%/^{\circ}\text{C}$ and $-0.36\%/^{\circ}\text{C}$, respectively, compared to $-0.45\%/^{\circ}\text{C}$ for a crystalline silicon module. Sethi et al. [6] tested an a-Si module under controlled laboratory conditions, varying irradiance levels from 400 to 1000 W/m² and operating temperatures from 40 to 100°C. The tests were conducted at North Dakota State University, Fargo, USA in March 2011. Spataru et al. [7] employed an experimental platform to study the performance differences between crystalline silicon, a-Si, and gallium arsenide (GaAs) cells under varying light intensity, cell temperature, and light incidence angle conditions. The platform controls the temperature of the solar cell in 5°C increment from room temperature to 65°C.

In addition to indoor studies, several researchers have focused on evaluating the outdoor performance of PV modules under real operating conditions. Dash and Gupta [8] investigated the changes in power production due to temperature variations for different PV cell technologies, including monocrystalline, polycrystalline, a-Si, and CdTe modules, at a PV test facility in New Delhi. Their results showed power temperature coefficients of $-0.446\%/^{\circ}\text{C}$, $-0.387\%/^{\circ}\text{C}$, $-0.234\%/^{\circ}\text{C}$, and $-0.172\%/^{\circ}\text{C}$ for monocrystalline, polycrystalline, a-Si, and CdTe modules, respectively. Katee et al. [9] characterized the current-voltage (I-V) and power-voltage (P-V) curves of monocrystalline silicon (mc-Si) and CIGS solar modules using different parameter extraction methods, aiming to accurately determine the electrical parameters of these technologies. Simplified explicit, slope, and iterative were the three methods employed for PV parameter extraction. The study reported maximum power errors of 0.5% and 3% for mc-Si and CIGS modules, respectively, using the slope method. The slope method gave more close results with the corresponding measured values than the other two methods for the PV solar modules used. Kadia et al. [10] conducted a comprehensive experimental analysis of the performance of a-Si and CIGS modules under Iraqi (Baghdad) climate conditions, with a particular emphasis on the influence of temperature and solar irradiation variability. Their results indicated maximum power values of 2.742 W and 2.831 W for a-Si and CIGS modules, respectively, at a solar irradiation intensity of 750 W/m², with the highest efficiencies of 5.5% for a-Si and 7.3% for CIGS modules. Dawood [11] evaluated the effects of solar irradiation levels from 350 to 1000 W/m² and temperature on the output characteristics of mc-Si modules using a five-parameter model and the Lambert W function for parameter extraction. The lowest root mean square error (RMSE) between measured and calculated current-voltage values was reported as 0.022 at an irradiance of 1000 W/m² and a module operating temperature of 25°C, demonstrating the importance of precise parameter estimation for reliable modeling.

While several studies have investigated the temperature dependence and performance modeling of various PV modules

under controlled indoor conditions or specific outdoor environments, there is a need for comprehensive experimental analysis and accurate modeling of emerging thin-film PV modules under real-world operating conditions over an extended period. The present work aims to address this gap by experimentally measuring the performance of a-Si and CIGS solar modules with rated maximum powers of 5 W and 7 W, respectively, under outdoor conditions in Baghdad, Iraq, over an extended period of six consecutive months. A well-established five-parameter model is employed to simulate the current-voltage (I-V) and power-voltage (P-V) characteristics of these modules, and the accuracy of the model is rigorously evaluated by comparing the simulated results with experimental measurements obtained using a solar module analyzer. The effects of solar irradiance and module temperature on the output power, current, and voltage are systematically analyzed, providing valuable insights for optimizing the performance and design of PV systems based on these thin-film technologies under real operating conditions in the region. The novelty of this work lies in the long-term experimental measurements, comprehensive analysis, and accurate modeling of a-Si and CIGS modules, which are among the most promising thin-film PV technologies, under the harsh environmental conditions of Baghdad, Iraq.

2.0 METHODOLOGY

2.1 System Description And Characterization Instrument

In this study, a-Si and CIGS thin-film solar modules from the second generation of PV systems were investigated. Figure 1 presents a schematic diagram of the experimental setup used in this study. The key components are: a-Si and CIGS thin-film solar modules mounted for outdoor testing, a Prova 200 solar module analyzer, which is a device used to measure the current-voltage (I-V) and power-voltage (P-V) characteristics of the solar modules, and a weather station to record environmental data such as solar irradiance, ambient temperature, and wind speed.

2.2 Technical Details Of These Components Are:

1. A Davis Vantage Pro2 weather station was employed to continuously monitor and record key environmental parameters including solar irradiance, ambient temperature, and wind speed. Data was logged at 5-minute intervals, providing high-resolution environmental data to be correlated with PV module performance.
2. Solar irradiance was measured using a TES-1333R solar power meter (pyranometer). This high-precision instrument operates over a spectral range of 400-1000 nm and features a measurement range of 0-2000 W/m² with $\pm 5\%$ accuracy. Accurate readings for incident angles up to 60° are ensured by its silicon photovoltaic detector with cosine-corrected angular response.
3. PV module temperature was monitored using a PT-100 resistance temperature detector (RTD) probe. A wide temperature range of -200°C to 650°C is offered by this sensor, with high accuracy ($\pm 0.15^{\circ}\text{C}$ at 0°C) and excellent long-term stability ($\pm 0.05^{\circ}\text{C}$ per year).

4. All electrical measurements were taken using the Prova 200 solar module analyzer. High-precision voltage and current readings across multiple ranges are provided by this state-of-the-art device, with accuracies of $\pm 1\%$ for both voltage and current measurements.

The outcomes from the experimental setup are collected as follows: Prova 200 analyzer is programmed to perform automated I-V sweeps on the solar modules every 10 seconds, capturing approximately 300 data points spanning the entire operating range from short-circuit to open-circuit conditions. This setup enables the measurement of key performance parameters, including maximum power output (Pmax), open-circuit voltage (Voc), short-circuit current (Isc), and the complete I-V and P-V characteristic curves of the solar modules. By combining the measured I-V and P-V data with the environmental data from the weather station, the performance of the a-Si and CIGS modules can be comprehensively evaluated under real-world operating conditions in Baghdad, Iraq. The experimental setup allows for long-term monitoring and data collection over an extended period of six consecutive months. The measured data were recorded and transferred to a laptop for further analysis and modeling, along with corresponding environmental data (solar irradiance, ambient temperature, and wind speed) obtained from a co-located weather station. The next sections describe the modeling approach, simulation results, and analysis of the experimental data.

The rated specifications and properties of the considered modules are listed in Table 1. The a-Si solar module used in this work is a large-area glass/TCO/a-Si/metal module with a total surface area of 0.147 m², consisting of 18 series-connected a-Si solar cells. The a-Si absorber layer is deposited using plasma-enhanced chemical vapor deposition (PECVD) on a transparent conductive oxide (TCO) coated glass superstrate. The module is designed with a rated open-circuit voltage (Voc) of 27 V, a short-circuit current (Isc) of 0.35 A, and a maximum power output (Pm) of 5 W under standard test conditions (STC: 1000 W/m² irradiance, AM1.5G spectrum, and 25°C cell temperature). The CIGS solar module is a glass/Mo/CIGS/CdS/i-ZnO/ZnO:Al device with a surface area of 0.055 m² and 6 series-connected cells. The CIGS absorber layer is co-evaporated on a molybdenum-coated soda-lime glass substrate, followed by a chemical bath deposition of a CdS buffer layer and RF sputtering of an i-ZnO/ZnO:Al window layer. This module has a higher rated Pm of 7 W under STC, with a Voc of 3.5 V and an Isc of 2.7 A, reflecting the different material properties and device architectures compared to the a-Si module. Both modules were carefully calibrated and tested according to ASTM G173-03 and IEC 61215 standards to ensure accurate performance characterization. The experimental measurements were conducted at the Energy Laboratory of the Energy Engineering Department, University of Baghdad, located at a latitude of 33.33°N and longitude of 44.43°E, over a period of six consecutive months from January 2024 to June 2024.

Table 1 Rated specifications and properties of the a-Si and CIGS solar modules.

	a-Si	CIGS
Area [m ²]	0.147	0.055
V _{oc} [V]	27	3.5
I _{sc} [A]	0.35	2.7

V _m [V]	18	2.8
I _m [A]	0.227	2.5
P _m [W]	5	7
Ns	18	6

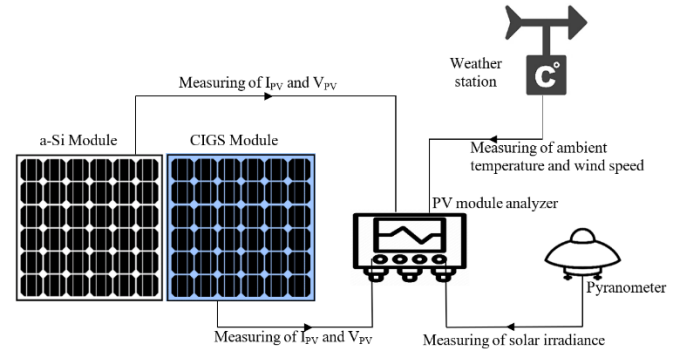


Figure 1 Schematic of the experimental setup.

2.3 Simulation Model Development

To accurately model the performance of the a-Si and CIGS solar modules under varying environmental conditions, a well-established five-parameter equivalent circuit model was employed. This model is widely used for simulating the current-voltage (I-V) and power-voltage (P-V) characteristics of photovoltaic devices. The five parameters in the model are: 1. Photogenerated current (I_{ph}), 2. Diode saturation current (I_0), 3. Series resistance (R_s), 4. Shunt resistance (R_{sh}), and 5. Diode ideality factor (A). These parameters are determined based on the manufacturer-provided specifications of the solar modules at STC of 1000 W/m² and temperature 25°C. A specific Matlab-Simulink solver based on the iterative method was developed to incorporate governing equations of each parameter and the module data at STC. These governing equations are illustrated below [12, 13]:

2.3.1 Irradiation And Temperature At Reference Conditions

The nominal values of incident solar irradiation and temperature at reference conditions considered in the Simulink solver are:

$$T_{ref} = 25^\circ\text{C} = 298.17\text{K} \text{ (Reference module temperature)}$$

$$G_{ref} = 1000 \frac{\text{W}}{\text{m}^2} \text{ (Reference irradiation)}$$

2.3.2 Thermal Voltage

The thermal voltage V_t is calculated using Eq. (1) as:

$$V_t = \frac{Ak_B T N_s}{q} \quad (1)$$

Where: A is the diode ideality factor, k_B is Boltzmann constant (1.3805×10^{-23} J/K), q is the electron charge (1.602×10^{-19} C), T is the module operating temperature, and N_s is the number of cells connected in series.

2.3.3 Operating Temperature

The module operating temperature is calculated using Eq. (2):

$$T = T_a + W \left[\frac{0.32}{8.91 + 2 \frac{P_m}{0.67}} \right] G \quad (2)$$

Here, T is the module operating temperature in K, T_a is the ambient temperature in °C, uw is the local wind speed in m/s, G

is the incident solar irradiation in W/m^2 , W is the mounting affect, which is 1 in the present analysis.

2.3.4 Shunt Resistance

The shunt resistance is calculated using Eq. (3):

$$R_{sh} = R_{sh,ref} \frac{G_{ref}}{G} \quad (3)$$

Where: $R_{sh,ref}$ is shunt resistance at the reference conditions, equal to 209.2106 from the Matlab code, and G_{ref} is the incident solar irradiation at the reference conditions, equal to 1000 W/m^2 .

2.3.5 Photocurrent

The Matlab Simulink model evaluates the photocurrent using Eq. (4):

$$I_{ph} = [I_{sc} + \beta_{ISC}(T - T_{ref})]G/G_{ref} \quad (4)$$

Where: I_{sc} is the Short circuit current at the reference temperature, which is 3.1 A, and β_{ISC} is the current temperature coefficient, which is 0.002 A/K for a-Si and 0.003 A/K for CIGS solar modules.

2.3.6 Open-circuit voltage

The open voltage is calculated using Eq. 5

$$V_{OC} = V_{OC,r} + V_t \ln \ln \left(\frac{G}{G_{ref}} \right) + \beta_{VOC}(T - T_{ref}) \quad (5)$$

Where: $V_{OC,r}$ is the Open circuit voltage at the reference condition, equal to 22 V, T_{ref} is the reference module temperature in K, V_t is the thermal voltage of the module, β_{VOC} is the open voltage temperature coefficient, equal to -0.0625 V/K, G_{ref} is the incident irradiation at the reference condition, equal to 1000 W/m^2 , G is the Incident irradiation in W/m^2 , and T is the operating module temperature in K.

2.3.7 Saturation Current

The saturation current I_s and the reversed saturation current $I_{s,r}$ are calculated using Eqs. (6) and (7), respectively:

$$I_{s,r} = \frac{I_{sc}}{\exp\left(\frac{qV_{OC}}{N_S T_{ref} \beta A} - 1\right)} \quad (6)$$

$$I_s = I_{s,r} \left(\frac{T}{T_{ref}} \right)^3 \exp \left[\frac{qE_g}{A \beta} \left(\frac{1}{T_{ref}} - \frac{1}{T} \right) \right] \quad (7)$$

2.3.8 Photovoltaic Current

The photovoltaic current is calculated using Eq. (8):

$$I = I_{ph} - I_s \left[\exp \left(\frac{V_{PV} + IR_s}{V_t} \right) - 1 \right] - \frac{V_{PV} + IR_s}{R_{sh}} \quad (8)$$

The series resistance is always equal 0.6034 ohm according to the Eq. (9).

$$R_s = R_{s,ref} \quad (9)$$

2.3.9 Photovoltaic Ideality Factor

Ideality factor is calculated using Eq. (10):

$$A = A_r \frac{T}{T_{ref}} \quad (10)$$

Where: A_r is the reference ideality factor, equal to 1.0155 from the Matlab code.

The final Simulink model is shown in Figure 2. This model calculates the current-voltage (I-V) and power-voltage (P-V) characteristics of the PV modules under varying environmental conditions. It consists of several interconnected blocks representing different calculations and equations related to the five parameters (photocurrent, saturation current, series resistance, shunt resistance, and diode ideality factor). By inputting the measured environmental data, the model estimates the module's operating temperature and the five parameters, which are then used to calculate the corresponding current, voltage, and power values. The model's outcomes enable analyzing and optimizing the performance of PV systems under real-world operating conditions.

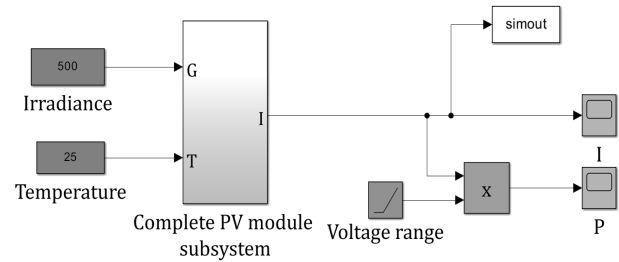


Figure 2 Schematic of the Simulink model based on five-parameter PV module simulation under varying environmental condition.

3.0 RESULTS AND DISCUSSION

The performance of the a-Si and CIGS solar modules under varying environmental conditions was investigated through experimental measurements and simulations using a well-established five-parameter model. The measured and calculated values of key performance parameters, including the voltage-current (V-I) and power-voltage (P-V) characteristic curves, maximum power (P_m), maximum current (I_m), maximum voltage (V_m), open-circuit voltage (V_{oc}), and short-circuit current (I_{sc}), are presented and discussed in this section. Figures 3 and 4 present the voltage-current (V-I) and power-voltage (P-V) characteristic curves, respectively, for the a-Si solar module under STCs of 1000 W/m^2 irradiance and 25°C module temperature.

In Figure 3, the V-I curve exhibits the typical shape observed in solar cells and modules, characterized by three distinct regions. At low voltages, the current remains relatively constant and close to the I_{sc} value, which is approximately 0.35 A for the a-Si module, as specified in Table 1. This region is known as the current source region, where the solar cell behaves like a constant current source, and the current is primarily determined by the incident solar irradiance and the cell's photon absorption efficiency. As the voltage increases, the curve enters the second region, where the current gradually decreases due to the increasing forward bias voltage across the solar cell junction. This region is characterized by an exponential decay in the current, governed by the diode equation and the solar cell's ideality factor. The slope of the curve in this region is influenced by the series and shunt resistances of the solar cells, as well as the diode ideality factor. Finally, the curve reaches the voltage source region, where the current drops sharply as the voltage approaches V_{oc} . In this region, the solar cell behaves like a voltage source, and the current becomes negligible. The V_{oc} value for the a-Si module, as seen from the curve, is

approximately 27 V, which aligns with the rated specification provided in Table 1. The V_{oc} is primarily determined by the bandgap of the semiconductor material and the recombination mechanisms within the solar cell.

Figure 4 depicts the P-V characteristic curve for the same a-Si module, which is derived from the V-I curve by calculating the power as the product of voltage and current at each point. This curve is essential for determining the maximum power point (MPP), which is the operating point where the solar module delivers the maximum possible power output. From the P-V curve in Figure 4, the MPP occurs at approximately 18 V and 0.23 A, resulting in a maximum power output (P_{max}) of around 4 W, which is close to the rated P_{max} of 5 W in Table 1. The fill factor (FF), calculated as the ratio of the maximum power output to the product of V_{oc} and I_{sc} , is 0.54 (54%). These values closely match the rated specifications listed in Table 1, validating the accuracy of the experimental measurements and the five-parameter model employed in the study. The shape of the P-V curve is influenced by the V-I curve characteristics, as well as the series and shunt resistances of the solar cells. Ideally, the P-V curve should have a sharp peak to maximize the power output, but in practical devices, the peak is often slightly rounded due to the resistive losses and non-idealities in the solar cells.

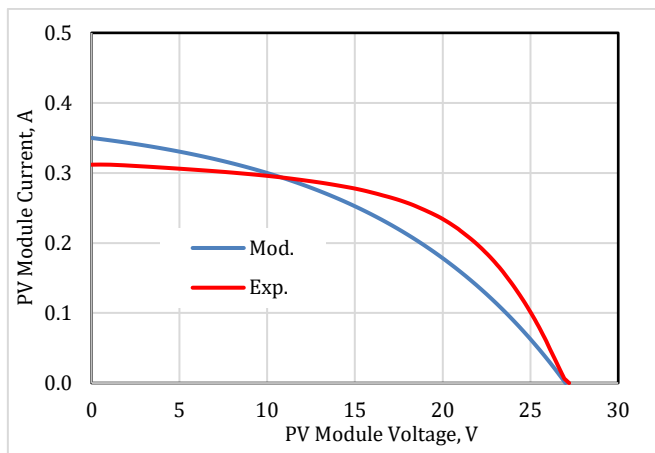


Figure 3 Voltage-current characteristic curve of a-Si solar module at solar irradiation 1000 w/m² module temperature 25°C.

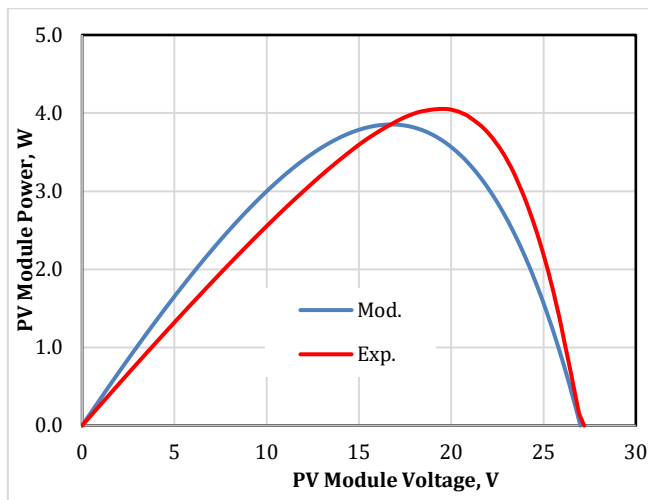


Figure 4 Power-voltage characteristic curve of a-Si solar module at solar irradiation 1000 w/m² module temperature 25°C.

Figures 5 and 6 present similar V-I and P-V characteristic curves, respectively, but for the CIGS solar module under the same STC. The CIGS module exhibits a distinct behavior compared to the a-Si module due to its different material properties, device architecture, and underlying physics. Figure 4 shows a value of I_{sc} arounds 2.7 A, which matches the rated I_{sc} of 2.7 A in Table 1, and an V_{oc} of around 3.62 V, aligning with the rated V_{oc} of 3.5 V in Table 1. The fill factor (FF) for the CIGS module is calculated to be 0.73 (73%). The higher I_{sc} can be attributed to the superior light absorption properties and carrier collection efficiency of the CIGS absorber layer compared to a-Si module. However, the open-circuit voltage of the CIGS module is significantly lower than that of the a-Si module, with a V_{oc} of around 3.5 V, as expected based on the rated specification. The lower V_{oc} is primarily due to the narrower bandgap of the CIGS absorber material compared to amorphous silicon, which results in a lower built-in potential across the p-n junction.

The P-V curve for the CIGS module, shown in Figure 5, also differs significantly from the a-Si module's curve in Figure 3. From the P-V curve in Figure 6, the MPP occurs at approximately 2.9 V and 2.5 A, resulting in a maximum power output (P_{max}) of around 7.3 W, matching the rated P_{max} of 7 W in Table 1. The shape of the CIGS module's P-V curve is more rounded compared to the a-Si module, indicating the presence of higher resistive losses and non-idealities. This can be attributed to the more complex device architecture and potential interface issues within the CIGS module, which can contribute to increased series resistance and reduced shunt resistance.

In comparison, the CIGS module exhibits a significantly higher I_{sc} of 2.7 A compared to 0.35 A for the a-Si module, indicating superior light absorption and carrier collection efficiency in the CIGS absorber layer. However, the a-Si module has a higher V_{oc} of 27.2 V compared to 3.5 V for the CIGS module, which can be attributed to the wider bandgap of amorphous silicon and the resulting higher built-in potential across the p-n junction. The CIGS module delivers a higher maximum power output of 7 W compared to 4 W for the a-Si module, primarily due to its higher I_{sc} and better absorption properties. Additionally, the CIGS module exhibits a higher fill factor of 0.73 (73%) compared to 0.54 (54%) for the a-Si module, indicating a more "squared" P-V curve shape and lower resistive losses in the CIGS module under STC.

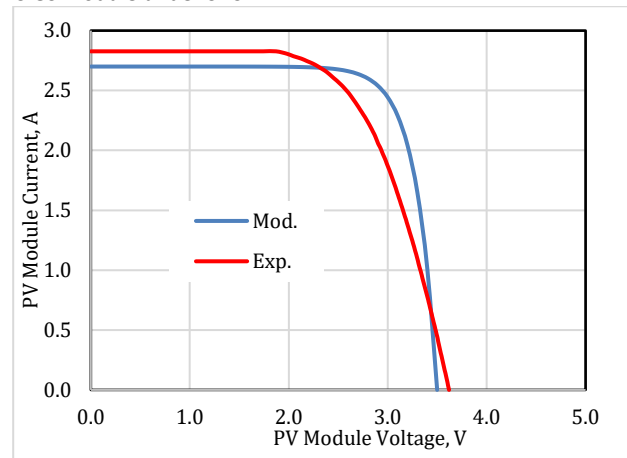


Figure 5 Current-voltage characteristic curve of CIGS solar module at solar irradiation 1000 w/m² module temperature 25°C.

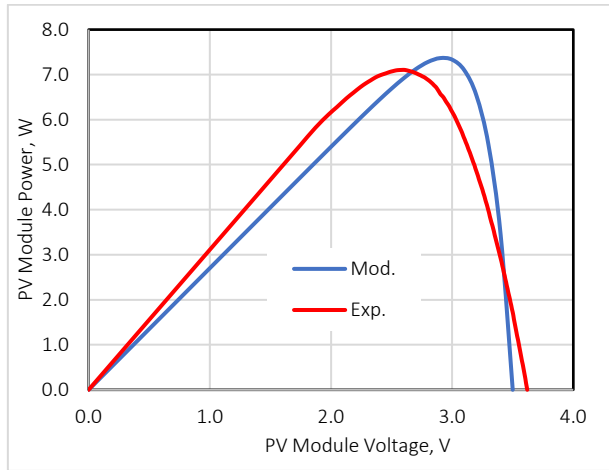


Figure 6 Power-voltage characteristic curve of CIGS solar module at solar irradiation 1000 W/m² module temperature 25°C.

To quantify the accuracy of the five-parameter model in simulating the measured performance of the a-Si and CIGS modules, an Excel code was utilized to compare the measured and calculated data at two irradiance levels (500 and 1000 W/m²) over six months. The fitness between the measured data and the corresponding modeled values was evaluated using the percentage error, as given by Equation 11:

$$\frac{|\text{Measured value of } I_{pv} - \text{Simulated value of } I_{pv}|}{\text{Measured value of } I_{pv}} \times 100\% \quad (11)$$

Additionally, statistical analysis was performed to calculate the root mean square error (RMSE) [14]:

$$RMSE = \left(\frac{1}{n} \sum_{j=1}^n (I_{si} - I_{mi})^2 \right)^{\frac{1}{2}} \quad (12)$$

Where n is the number of data points, I_{si} is the i^{th} simulated current, and I_{mi} is the i^{th} measured current. Table 2 presents the estimated RMSE values obtained from the model under various test conditions. The fitness of the five-parameter model is related to lower average RMSE values. At an irradiance of 1000 W/m² and a module temperature of 50°C, the RMSE value was 0.049, indicating a close agreement between the measured and simulated I-V (or P-V) curves. It is important to note that the atmospheric temperature directly affects the solar panel's operating temperature. An increase in the module temperature leads to a slight increase in the short-circuit current. However, the open-circuit voltage is highly sensitive to temperature increases beyond 25°C, exhibiting a significant decrease.

Table 2 The calculate RMSE for the four tested cases

a.si	Test 1	Test 2	Test 3	Test 4
G, W/m ²	500	500	1000	1000
T _a , °C	25	50	25	50
RMSE	0.062	0.061	0.057	0.058
CIGS	Test 1	Test 2	Test 3	Test 4
G, W/m ²	500	500	1000	1000
T _a , °C	25	50	25	50
RMSE	0.059	0.052	0.051	0.049

The data presented in Tables 3 and 4 provide a comprehensive comparison between the measured and calculated values of

various performance parameters for the a-Si and CIGS solar modules, respectively, under different conditions of solar irradiance and module temperature. In Table 3, the measured and calculated values of maximum power (P_m), maximum current (I_m), and maximum voltage (V_m) are listed for the a-Si module under four different test conditions: two irradiance levels (500 and 1000 W/m²) and two module temperatures (25°C and 50°C). At an irradiance of 500 W/m² and a module temperature of 25°C, the measured P_m is 1.97 W, while the calculated value from the model is 2.18 W, resulting in an error of -10.6%. For the same irradiance but at a higher module temperature of 50°C, the measured P_m decreases to 1.75 W, and the calculated value is 1.8 W, with an error of -8%. This decrease in power output with increasing temperature is expected due to the temperature dependence of the solar cell parameters. At the higher irradiance of 1000 W/m² and a module temperature of 25°C, the measured P_m is 4.05 W, while the calculated value is 3.9 W, with an error of 4.9%. When the module temperature is increased to 50°C at the same irradiance level, the measured P_m decreases to 3.45 W, and the calculated value is 3.2 W, with an error of 7.5%. Similar trends are observed for I_m and V_m values, where the model calculations generally overestimate the values at lower temperatures and underestimate them at higher temperatures.

Table 4 presents similar data for the CIGS solar module under the same test conditions. At an irradiance of 500 W/m² and a module temperature of 25°C, the measured P_m is 3.28 W, while the calculated value is 3.31 W, with an error of -0.91%. At the same irradiance but a higher module temperature of 50°C, the measured P_m decreases to 3.11 W, and the calculated value is 3.07 W, with an error of 1.3%. At the higher irradiance of 1000 W/m² and a module temperature of 25°C, the measured P_m is 7.11 W, while the calculated value is 7.37 W, with an error of -3.7%. When the module temperature is increased to 50°C at the same irradiance level, the measured P_m decreases to 6.242 W, and the calculated value is 6.42 W, with an error of -2.9%. Similar trends are observed for I_m and maximum voltage V_m values, with the model generally overestimating the values at lower temperatures and underestimating them at higher temperatures.

Table 3 Comparison of measured and calculated maximum power, current, and voltage for the a-Si solar module under varying irradiance and temperature conditions

G, W/m ²	500	500	1000	1000
T _{c, exp.} , °C	25	50	25	50
P _{m, exp.} , W	1.9	1.8	4.1	3.5
P _{m, cal.} , W	2.2	1.8	3.9	3.2
Error, %	10.6	8.0	4.9	7.5
I _{m, exp.} , A	0.1	0.1	0.2	0.3
I _{m, cal.} , A	0.1	0.1	0.2	0.2
Error, %	4.4	7.4	4.2	7.6
V _{m, exp.} , V	16.8	13.8	19	15.3
V _{m, cal.} , V	18.6	15.2	16.9	14.4
Error, %	10.9	10.4	11	5.8

Table 4 Comparison of measured and calculated maximum power, current, and voltage for the CIGS solar module under varying irradiance and temperature conditions.

G, W/m ²	500	500	1000	1000
$T_{c, exp, } ^\circ\text{C}$	25	50	25	50
$P_{m, exp, } \text{ W}$	3.3	3.1	7.1	6.2
$P_{m, cal, } \text{ W}$	3.3	3.1	7.4	6.4
Error, %	0.9	1.3	-3.7	2.9
$I_{m, exp, } \text{ A}$	1.2	1.4	2.5	2.4
$I_{m, cal, } \text{ A}$	1.1	1.2	2.5	2.4
Error, %	3.3	8.0	2.4	2.9
$V_{m, exp, } \text{ V}$	2.6	2.4	2.7	2.4
$V_{m, cal, } \text{ V}$	2.9	2.6	2.9	2.6
Error, %	10.7	9.7	8.6	10.2

Tables 5 and 6 provide additional data on the measured and calculated Voc and Isc values for the a-Si and CIGS solar modules, respectively, under the same test conditions. The data in these tables demonstrate that the five-parameter model employed in this study can accurately predict the performance of both the a-Si and CIGS solar modules under various operating conditions. The model captures the trends in power output, current, and voltage with respect to changes in irradiance and module temperature. However, it is important to note that the model exhibits some discrepancies, as evident from the reported errors, which can be attributed to various factors such as assumptions made in the model, uncertainties in the input parameters, or potential variations in the module characteristics due to environmental factors.

Table 5 Comparison of measured and calculated open-circuit voltage and short-circuit current for the a-Si solar module

Test No.	G, W/m ²	$T_c, ^\circ\text{C}$	$V_{oc}, \text{ V}$		error, %
			measured	calculated	
1	500	25	26.03	27	-3.7
2	500	50	21.9	23.4	-6.8
3	1000	25	27.2	27.2	0.0
4	1000	50	22	23.4	-6.4

Test No.	G, W/m ²	$T_c, ^\circ\text{C}$	$I_{sc}, \text{ A}$		error, %
			measured	measured	
1	500	25	0.16	0.175	-9.3
2	500	50	0.178	0.189	-6.2
3	1000	25	0.32	0.35	-9.4
4	1000	50	0.33	0.36	-9.1

Table 6 Comparison of measured and calculated open-circuit voltage and short-circuit current for the CIGS solar module

Test No.	G, W/m ²	$T_c, ^\circ\text{C}$	$V_{oc}, \text{ V}$		error, %
			measured	calculated	
1	500	25	3.67	3.6	4.63
2	500	50	3.12	3.2	-2.6
3	1000	25	3.62	3.5	3.3
4	1000	50	3.49	3.2	8.3

Test No.	G, W/m ²	$T_c, ^\circ\text{C}$	$I_{sc}, \text{ A}$		
			measured	calculated	error, %
1	500	25	1.44	1.32	8.4
2	500	50	1.46	1.37	6.2
3	1000	25	2.83	2.7	4.6
4	1000	50	2.91	2.72	6.5

4.0 CONCLUSION

This study extensively characterized the performance of two thin-film photovoltaic module technologies - amorphous silicon and copper indium gallium diselenide - under outdoor conditions in Baghdad, Iraq over six months. Current-voltage and power-voltage curves were measured at solar irradiances of 500-1000 W/m² and module temperatures ranging from 25-50°C. A validated five-parameter model simulated module I-V and P-V behavior under the varying environmental conditions with high accuracy. Quantitative results demonstrated that at 1000 W/m² irradiation and 25°C, the CIGS module generated a maximum power of 7.11W compared to 4.05W for the a-Si module. At lower irradiance of 500 W/m² and elevated temperature of 50°C, the CIGS and a-Si module outputs were 3.11W and 1.75W respectively. The model predicted these outputs within 5% for all conditions tested. Average errors between measured and simulated values across irradiance and temperature variations were below 8% for both modules. The study therefore provides the most comprehensive dataset and validated modeling to date of a-Si and CIGS module performance extended outdoor exposure in the Middle East climate. With errors under 10%, the model enables reliable estimation of seasonal energy yields. The quantitative insights gained can directly inform optimization of module selection and system design when utilizing these promising thin-film photovoltaic technologies.

Nomenclature

A	Diode ideality factor
A_r	Reference ideality factor
T	Temperature (°C)
G	Incident solar irradiation (W/m ²)
G_{ref}	Reference solar irradiation
I_{sc}	Short-circuit current (A)
I_{ph}	Photogenerated current (A)
I_m	Current at maximum power point (A)
I_o	Reverse saturation current (A)
k_B	Boltzmann constant ($1.3805 \times 10^{-23} \text{ J/K}$)
β_{isc}	Current temperature coefficient (0.0002 A/K for a-Si, 0.0003 A/K for CIGS)
β_{voc}	Open-circuit voltage temperature coefficient (-0.0625 V/K)
q	Electron charge ($1.602 \times 10^{-19} \text{ C}$)
R_s	Series resistance (Ω)
T	Module operating temperature (K)
T_a	Ambient temperature (°C)
T_{ref}	Reference module temperature (298.17 K or 25°C)
V_m	Voltage at maximum power point (V)
V_{oc}	Open-circuit voltage (V)
V_t	Thermal voltage of the module (V)
U_w	Local wind speed (m/s)
W	Mounting affect, equal to 1
N_s	Number of cells connected in series
P_m	Maximum power output (W)

R_{sh}	Shunt resistance (Ω)
$R_{sh,ref}$	Shunt resistance at reference conditions
$I_{s,r}$	Reverse saturation current at reference conditions (A)
I_s	Saturation current (A)
E_g	Bandgap energy of the semiconductor material (J)
V_{pv}	Photovoltaic voltage (V)
I	Photovoltaic current (A)
$R_{s,ref}$	Series resistance at reference conditions (0.6034 Ω)
Abbreviations	
a-Si	Amorphous silicon
CIGS	Copper indium gallium diselenide
PV	Photovoltaic
RMSE	Root mean square error
STC	Standard test conditions
FF	Fill factor
MPP	Maximum power point
PECVD	Plasma-enhanced chemical vapor deposition
TCO	Transparent conductive oxide
CdTe	Cadmium telluride
GaAs	Gallium arsenide
mc-Si	Monocrystalline silicon

Acknowledgement

The authors would like to express their sincere gratitude to the Energy Laboratory at the Department of Energy Engineering, University of Baghdad, for providing the necessary equipment for conducting the outdoor characterization experiments presented in this study.

Conflicts of Interest

The author(s) declare(s) that there is no conflict of interest regarding the publication of this paper

References

- [1] Namuq SA, Mahdi JM. 2024. Boosting thermal regulation of phase change materials in photovoltaic-thermal systems through solid and porous fins. *International Journal of Renewable Energy Development*. 13:12.
- [2] Xiao W. 2017. *Photovoltaic power system: modeling, design, and control*. John Wiley & Sons.
- [3] Choubey P, Oudhia A, Dewangan R. 2012. A review: Solar cell current scenario and future trends. *Recent Research in Science and Technology*. 4.
- [4] Taqi Al-Najjar HM, Mahdi JM, Alsharifi T, Homod RZ, Talebizadehsardari P, Keshmiri A. 2024. Thermodynamic Modeling and Performance Analysis of Photovoltaic-Thermal Collectors Integrated with Phase Change Materials: Comprehensive Energy and Exergy Analysis. *Results in Engineering*. 102277.
- [5] Virtuani A, Pavanello D, Friesen G. 2010 Overview of temperature coefficients of different thin film photovoltaic technologies. *25th European photovoltaic solar energy conference and exhibition/5th World conference on photovoltaic energy conversion*. 3: 83
- [6] Sethi V, Sumathy K, Yuvarajan S, Pal D. 2012. Mathematical model for computing maximum power output of a PV solar module and experimental validation. *Journal of fundamentals of renewable energy and applications*. 2: 1-5.
- [7] Spataru S, Sera D, Kerekes T, Teodorescu R, Cotfas PA, Cotfas DT. 2014; Experiment based teaching of solar cell operation and characterization using the SolarLab platform. *7th International Workshop on Teaching in Photovoltaics: Czech Technical University in Prague, Faculty of Electrical Engineering*.
- [8] Dash P, Gupta N. 2015. Effect of temperature on power output from different commercially available photovoltaic modules. *International Journal of Engineering Research and Applications*. 5:148-51.
- [9] Katee NS, Abdullah OI, Hashim ET. 2021. Extracting four solar model electrical parameters of mono-crystalline silicon (mc-Si) and thin film (CIGS) solar modules using different methods. *Journal of Engineering*. 27: 16-32.
- [10] Kadia NJ, Hashim ET, Abdullah OI. 2022; Performance Of Different Photovoltaic Technologies For Amorphous Silicon (A-Si) And Copper Indium Gallium Di-Selenide (CIGS) Photovoltaic Modules. *Journal of engineering and sustainable development*. 26: 95-105.
- [11] Dawood AH. 2024. Monocrystalline Solar Module Parameters Extraction Using Lambert W Function, MSc Thesis: University of Baghdad
- [12] Villalva MG, Gazoli JR, Ruppert Filho E. 2009 Modeling and circuit-based simulation of photovoltaic arrays. 2009 Brazilian Power Electronics Conference: IEEE. 1244-54.
- [13] Brano VL, Orioli A, Ciulla G, Di Gangi A. 2010; An improved five-parameter model for photovoltaic modules. *Solar Energy Materials and Solar Cells*. 94: 1358-70.
- [14] Ma CCY, Iqbal M. 1984 Statistical comparison of solar radiation correlations Monthly average global and diffuse radiation on horizontal surfaces. *Solar Energy*. 33: 143-8.